Anisotropic line tension of domains in lipid monolayers

E. Velasco*
Departamento de Física Teórica de la Materia Condensada, Instituto de Física de la Materia Condensada (IFIMAC) and Instituto de Ciencia de Materiales Nicolás Cabrera, Universidad Autónoma de Madrid, E-28049 Madrid, Spain

L. Mederos†
Instituto de Ciencia de Materiales de Madrid, Consejo Superior de Investigaciones Científicas, C/Sor Juana Inés de la Cruz, 3, E-28049 Madrid, Spain

(Received 22 May 2019; published 27 September 2019)

We formulate a simple effective model to describe molecular interactions in a lipid monolayer and calculate the line tension between coexisting domains. The model represents lipid molecules in terms of two-dimensional anisotropic particles on the plane of the monolayer. These particles interact through forces that are believed to be relevant for the understanding of fundamental properties of the monolayer: van der Waals interactions originating from lipid chains and dipolar forces between dipole groups in the molecular heads. The model stresses the liquid-crystalline nature of the ordered phase in lipid monolayers and explains coexistence properties between ordered and disordered phases in terms of molecular parameters. Thermodynamic and interfacial properties of the model are analyzed using density-functional theory. In particular, the line tension at the interface between ordered and disordered phases turns out to be highly anisotropic with respect to the angle between the nematic director and the interface separating the coexisting phases. This important feature mainly results from the tilt angle of lipid chains and, to a lesser extent, from dipolar interactions perpendicular to the monolayer. The role of the two dipolar components, parallel and perpendicular to the monolayer, is assessed by comparing with computer simulation results for lipid monolayers.

DOI: 10.1103/PhysRevE.100.032413

I. INTRODUCTION

Lipid monolayers have been intensely investigated in the past decades because of their importance as paradigms for various interfacial problems of biological importance, in particular, for the lung surfactant system [1,2]. Monolayers made of one- or multicomponent lipid molecules at the air-liquid water interface are considered to be useful models for a lipid monolayer. One of the more extensively analyzed lipid monolayers consists of 1,2-dipalmitoyl-*sn*-glycero-3-phosphocholine (DPPC) molecules and mixtures with similar molecules of different saturation degrees in their aliphatic chains. Below some critical point, pure and mixed monolayers generally show phase separation between a phase with disordered chains or a liquid-expanded (LE) (fluid) phase and a phase with ordered chains or a liquid-condensed (LC) (gel- or solidlike) phase [3,4].

The molecular structure in the LC phase consists of molecules with straight and tightly packed molecular chains. Molecules show a high degree of positional order, compatible with a global or local two-dimensional crystal or glassy state [3], although the precise molecular ordering is open to debate (see, for example, Ref. [5] where ordered domains in bilayers of lipid mixtures are observed to be composed of subdomains with different orders). In the LE phase, by contrast, not only the chains, but also the molecular centers of mass are disordered. Also, molecular chains in both phases are observed to be tilted with respect to the monolayer normal to some degree [3,6,7]. The tilt is believed to optimize chain contact and van der Waals interactions [8]. In the case of the LC phase, the optimal contact energy compensates for the decrease in entropy associated with the positional molecular ordering. The LC-LE phase transition can conceptually be regarded as a classical first-order phase transition between two-dimensional phases, one possessing some kind of orientational and positional order and the other exhibiting orientational and positional disorder, such as in a standard liquid.

Lipid molecules are amphiphilic in nature, i.e., they show polar and nonpolar characteristics that explain their tendency to occupy the liquid interface. These characteristics may play slightly different roles in the two-dimensional phase transitions. The nonpolar part, through the condensation and ordering of the molecular chains, do clearly play the most important role in the phase transition, but less is known about the role of the polar heads. Experimental investigation of this problem [7,9–12] is difficult, and some important questions about lipid domains at the phase transition are still open, for example, the intricate domains shapes, the domain structure, the stability, and the growth kinetics of domains at coexistence. The very role played by the polar and nonpolar interactions on the above properties is uncertain.

From the theoretical side, progress has been slow. To date, theoretical models have been formulated mostly at the mesoscopic level and incorporate polar and nonpolar interactions between molecules more or less implicitly [13–17]. Models have focused on the understanding of domain shape

*enrique.velasco@uam.es
†lmederos@icmm.csic.es

and domain-shape transitions, taking thermodynamic coexistence as given. But thermodynamically consistent *microscopic* models that start from an interaction potential energy are scarce and not fully satisfactory: Existing models are formulated on lattices and do not include dipolar interactions [18,19]. More complete models, in the tradition of classical liquid-state theory, are more powerful in that, not only bulk thermodynamics (and, therefore, phase transitions), but also interface thermodynamics and structural information, can be calculated. This information may be very useful as an input to mesoscopic models or to understand computer simulations.

In the present paper, we formulate a simple microscopic model based on interacting two-dimensional effective anisotropic particles. The model is inspired by recent computer simulation results that use atomistic force fields [20,21]. The model includes van der Waals interactions between lipid chains and dipolar forces with perpendicular and parallel components with respect to the monolayer associated with polar interactions between lipid head groups. Using density-functional theory (DFT) and assuming that the LC phase can be assimilated into a liquid-crystalline fluid nematic phase [22], we obtain phase diagrams for different values of interaction parameters. In particular, we study their effect on the density gap between coexisting domains. Also, the theory allows for the study of the microscopic structure at the interface separating the two coexisting domains and the molecular orientation at the interface. The line tension turns out to be strongly anisotropic with respect to this orientation. The importance of line-tension anisotropy has been stressed before in relation to lipid domains in monolayers [23]. Our microscopic model makes definite predictions about this anisotropy in terms of parameters that have a molecular basis. The model focuses on the orientational properties, i.e., the nematic liquid-crystalline aspect, of the molecules in the LC phase [22]. Contributions from any possible positional order are neglected. Since positional order is believed to have glassy or local characteristics [3,5], it seems sensible to believe that the orientational order will give a larger contribution to the value and anisotropicity of the line tension than positional order.

Our results have implications at various levels. First, we conclude that the model correctly reproduces the molecular orientation at the LC domain boundaries if the in plane component of molecular dipoles is absent. Therefore, our results support the concept that this dipolar component should play no role in determining the structure. This conclusion is in agreement with the atomistic simulation results [21]. Second, the dipolar component perpendicular to the monolayer does not essentially perturb molecular orientation at the boundary, although it substantially lowers the line tension. Also, anisotropicity of the line tension with respect to molecular orientation at the boundary, already present in the absence of any dipolar interaction, is reinforced by the presence of a perpendicular dipole. The anisotropic nature of the line tension is an essential prediction of the model, and we argue that it should be incorporated in mesoscopic models for domain shape.

II. THEORETICAL SECTION

Some features of our two-dimensional effective model for a lipid monolayer are inspired by the recent simulation study [20] of an atomistic model for a DPPC monolayer. In this reference, the density of interaction units of a molecule, projected on the plane of the monolayer, was studied separately for domains of the LC and LE phases. A histogram of projected molecular aspect ratios was obtained where the aspect ratio was defined from the two gyration radii of the projected interaction units of the molecules. Despite the different chain orderings in the LC and LE domains, the respective histograms result in mean aspect ratios very close to 2.5 in both phases. This means that the average shape of a lipid molecule, projected on the plane of the monolayer, is close to that of an ellipse with the latter aspect ratio, Fig. 1. Admittedly, the distribution of aspect ratio obtained in the simulation is quite broad since the tilt angle of the molecular chains also fluctuates about an average value. In a more complete model, the width of the distribution could be accounted for by assuming that our two-dimensional effective particles have an aspect-ratio polydispersity. The effect of length polydispersity has been shown to play a crucial role in phase equilibria involving phases with partial spatial order [24]. However, its impact on the isotropic-nematic phase transition is not expected to be crucial at the present level of modeling.

Based on these results, in the present model, we assume that our two-dimensional effective particles consist of identical rectangular particles with an aspect ratio of 3. The reason why a rectangular, rather than elliptical, shape is chosen, and for the value of aspect ratio adopted, will become clear later on. The elongated projected shape of lipid molecules reflects the molecular geometry and the tendency of real lipid molecules to be slightly tilted with respect to the monolayer normal in both LC and LE phases. As regards the interaction between two molecules, the anisotropic shape captures the fact that side-to-side configurations have a shorter overlap distance than end-to-end configurations. Therefore, the effective particle interaction contains a purely repulsive term represented by a two-dimensional hard-rectangle (HR) potential for particles with length L and width σ_0 with $\kappa = L/\sigma_0 = 3$ as the aspect ratio.

Figure 1 shows the most representative effective-particle configurations. Let us associate a two-dimensional unit vector $\hat{\boldsymbol{e}}_i$ with the ith molecule. This vector is on the plane of the monolayer and points along the projection of the lipid tail. Therefore, it is parallel to the long axis of the effective two-dimensional particle. If $\hat{\boldsymbol{r}}$ is the unit vector joining particle 1 with 2, we define $a_i = \hat{\boldsymbol{r}} \cdot \hat{\boldsymbol{e}}_i$ and $b = \hat{\boldsymbol{e}}_1 \cdot \hat{\boldsymbol{e}}_2$. Then, the three end-to-end configurations have $(b, a_1, a_2) = (+1, +1, +1), (-1, \pm 1, \mp 1)$, whereas, for the two side-to-side configurations, $(b, a_1, a_2) = (+1, 0, 0)$ and $(-1, 0, 0)$. With the chain molecular structure in mind, it is clear that, as far as van der Waals interactions are concerned, the first two end-to-end configurations, $\rightarrow\rightarrow$ and $\rightarrow\leftarrow$, cannot have the same energy (note that the configurations $\rightarrow\leftarrow$ and $\leftarrow\rightarrow$ are taken as equivalent). Also, the two side-to-side configurations, $\uparrow\uparrow$ and $\uparrow\downarrow$, cannot have the same energy either. These two configurations contain the most important relative difference energetically: In the case of $b = +1$, lipid chains are in complete contact, whereas, in the second $b = -1$, they interact much less.

Thus, to the HR potential, an anisotropic attractive contribution between the effective particles is added. This

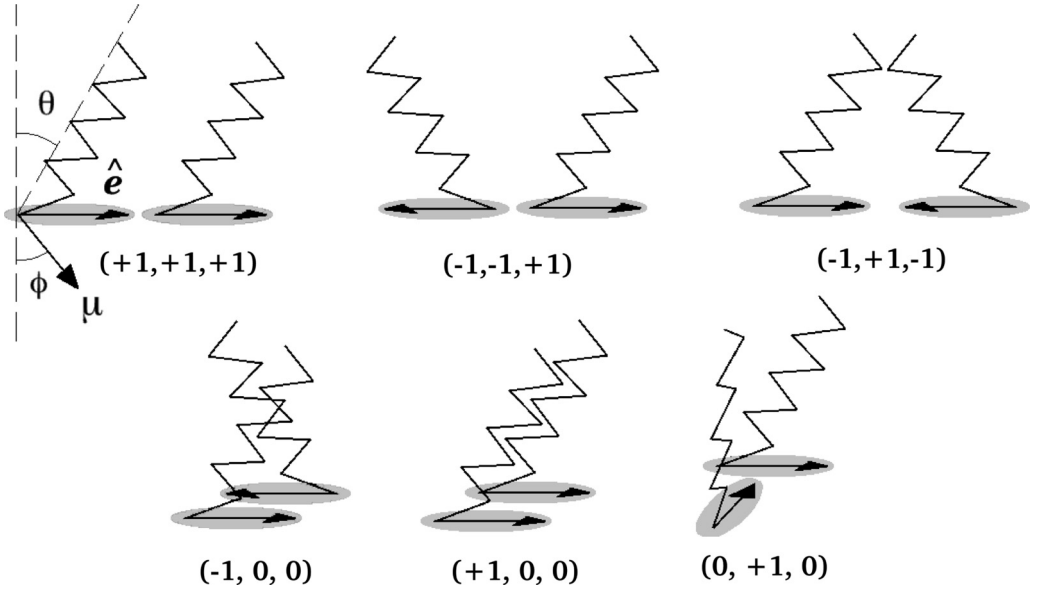

FIG. 1. Schematic of representative effective-particle configurations and corresponding lipid chain orientations. Numbers below each cartoon correspond to values of (b, a_1, a_2) (see the text for details).

contribution is intended to represent the van der Waals attraction between the lipid chains and should be sensitive to the sign of b. The model for the attractive interaction will be a modified Gay-Berne (MGB) potential [25]. The GB potential is an anisotropic Lennard-Jones-like potential which has been extensively studied in three-dimensional fluids to account for interactions between anisotropic mesogenic particles [26–28]. However, its use in two-dimensional systems is scarce, probably because it predicts a continuous, rather than first order, phase transition between isotropic and nematic fluids. Since the original GB model presents head-to-tail symmetry, it cannot discriminate between the two side-to-side (or end-to-end) configurations, and a modification is required to introduce an energy splitting between the configurations.

In the original GB model, the potential energy for two particles with relative center-of-mass vector $\boldsymbol{r} = \boldsymbol{r}_2 - \boldsymbol{r}_1$ and orientations $\hat{\boldsymbol{e}}_1$ and $\hat{\boldsymbol{e}}_2$ is

$$\Phi_{\mathrm{GB}}(\boldsymbol{r}, \hat{\boldsymbol{e}}_1, \hat{\boldsymbol{e}}_2) = 4\epsilon(\boldsymbol{r}, \hat{\boldsymbol{e}}_1, \hat{\boldsymbol{e}}_2,)f(\boldsymbol{r}, \hat{\boldsymbol{e}}_1, \hat{\boldsymbol{e}}_2), \tag{1}$$

with

$$\epsilon(\boldsymbol{r}, \hat{\boldsymbol{e}}_1, \hat{\boldsymbol{e}}_2) = \epsilon_{\mathrm{GB}}\epsilon_1^{\nu}(\hat{\boldsymbol{e}}_1, \hat{\boldsymbol{e}}_2)\epsilon_2^{\mu}(\hat{\boldsymbol{r}}, \hat{\boldsymbol{e}}_1, \hat{\boldsymbol{e}}_2), \tag{2}$$

and

$$f(\boldsymbol{r}, \hat{\boldsymbol{e}}_1, \hat{\boldsymbol{e}}_2) = \left(\frac{\sigma_0}{r - \sigma(\hat{\boldsymbol{r}}, \hat{\boldsymbol{e}}_1, \hat{\boldsymbol{e}}_2) + \sigma_0}\right)^{12} - \left(\frac{\sigma_0}{r - \sigma(\hat{\boldsymbol{r}}, \hat{\boldsymbol{e}}_1, \hat{\boldsymbol{e}}_2) + \sigma_0}\right)^{6}. \tag{3}$$

$\sigma(\hat{\boldsymbol{r}}, \hat{\boldsymbol{e}}_1, \hat{\boldsymbol{e}}_2)$ is a contact distance that depends on the relative particle angle $\hat{\boldsymbol{r}}$ and the two particle orientations $\hat{\boldsymbol{e}}_1, \hat{\boldsymbol{e}}_2$. ϵ_{GB} is an energy scale, whereas $\mu = 2$ and $\nu = 1$ are exponents. σ_0 is made to coincide with the particle width. In the standard Gay-Berne model, the contact distance is given by the hard-Gaussian overlap (HGO) model. The full expressions are as follows:

$$\begin{aligned}
\sigma(\hat{\boldsymbol{r}}, \hat{\boldsymbol{e}}_1, \hat{\boldsymbol{e}}_2) &= \sigma_{\mathrm{HGO}}(\hat{\boldsymbol{r}}, \hat{\boldsymbol{e}}_1, \hat{\boldsymbol{e}}_2) \\
&= \sigma_0\left\{1 - \frac{\chi}{2}\left[\frac{(a_1 + a_2)^2}{1 + \chi b} + \frac{(a_1 - a_2)^2}{1 - \chi b}\right]\right\}^{-1/2}, \\
\epsilon_1(\hat{\boldsymbol{e}}_1, \hat{\boldsymbol{e}}_2) &= \{1 - \chi^2 b^2\}^{-1/2}, \\
\epsilon_2(\hat{\boldsymbol{r}}, \hat{\boldsymbol{e}}_1, \hat{\boldsymbol{e}}_2) &= 1 - \frac{\chi'}{2}\left[\frac{(a_1 + a_2)^2}{1 + \chi' b} + \frac{(a_1 - a_2)^2}{1 - \chi' b}\right],
\end{aligned} \tag{4}$$

where $\sigma_{\mathrm{HGO}}(\hat{\boldsymbol{r}}, \hat{\boldsymbol{e}}_1, \hat{\boldsymbol{e}}_2)$ is the contact distance of the HGO model (which closely approximates that of hard ellipses). In the equations above, the parameter χ is related to the particle aspect ratio by $\chi = (\kappa^2 - 1)/(\kappa^2 + 1)$. Likewise, $\chi' = (\kappa'^{1/\mu} - 1)/(\kappa'^{1/\mu} + 1)$, where κ' is the ratio of potential energies in a T configuration and in a parallel configuration [25] (see below).

In our modified model, we introduce two variations to the standard GB model, Eqs. (4). The first is forced by the fact that the HGO model for the hard core does not produce a first-order phase transition between the isotropic and the nematic phases. As discussed, this is a necessary requirement for the model in our application to coexisting domains in the monolayer (note that the presence of an attractive contribution in the GB model does not modify this scenario). To correct this unwanted feature, we have modified the hard core and adopted a HR shape. This model is known to exhibit a first-order transition from the isotropic phase to the uniaxial nematic phase in a range of aspect ratios [29]. In particular, for an aspect ratio $\kappa = 3$, the phase transition is of first order and gives rise to a density gap with a sufficiently wide coexistence region. The modification involves substituting the contact distance in (4) by that of the HR model $\sigma(\hat{\boldsymbol{r}}, \hat{\boldsymbol{e}}_1, \hat{\boldsymbol{e}}_2) = \sigma_{\mathrm{HR}}(\hat{\boldsymbol{r}}, \hat{\boldsymbol{e}}_1, \hat{\boldsymbol{e}}_2)$.

The second modification involves splitting the energy of parallel $b = +1$ and antiparallel $b = -1$ configurations as discussed above. This is performed by modifying the ϵ_1 function

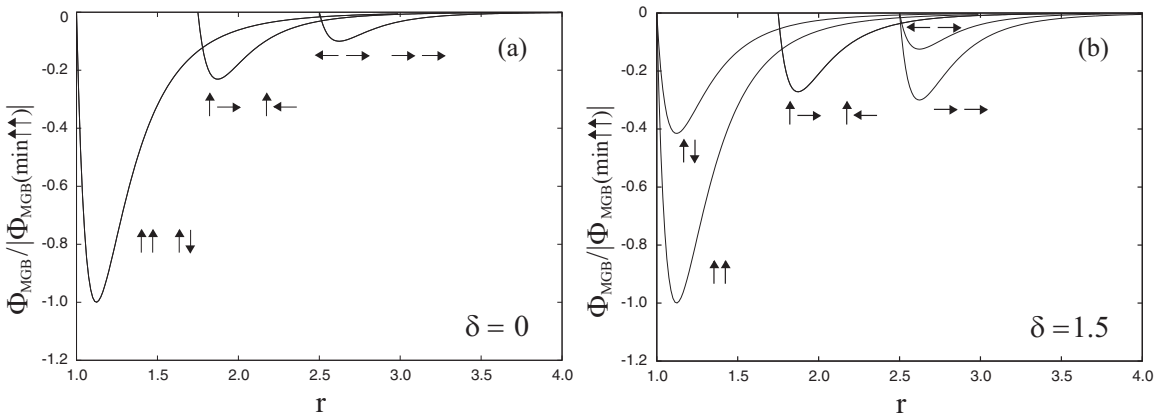

FIG. 2. The modified Gay-Berne potential for various relative configurations of two molecules. $\hat{\boldsymbol{e}}$ vectors for each configuration are indicated as arrows. Values of the parameters are $\kappa = 3$, $\kappa' = 0.3$, $\mu = 2$, and $\nu = 1$. (a) $\delta = 0$. (b) $\delta = 1.5$.

to

$$\epsilon_1(\hat{\boldsymbol{e}}_1, \hat{\boldsymbol{e}}_2) = \left\{1 - \tfrac{1}{2}\chi^2(1 + \delta b)\right\}^{-1/2}, \tag{5}$$

where δ is an asymmetry parameter that quantifies the energy splitting. The resulting modified potential (1) with (5) instead of (4) for the energy function ϵ_1 will be called the MGB potential $\Phi_{\rm MGB}(\boldsymbol{r}, \hat{\boldsymbol{e}}_1, \hat{\boldsymbol{e}}_2)$. Note that $\delta = 0$ does not reduce (5) to the standard GB model. This simple modification of the original expression in (4) introduces the necessary splitting between the parallel and the antiparallel configurations without spoiling the balance between the other important configurations.

Figure 2 shows the MGB potential for various selected relative configurations of two particles: The two side-to-side configurations $\uparrow\uparrow$ and $\uparrow\downarrow$, the two T configurations $\uparrow\leftarrow$ and $\uparrow\rightarrow$, and the two side-to-side configurations $\rightarrow\rightarrow$ and $\rightarrow\leftarrow$. The parameter κ' describes the relative energy between parallel and T configurations in the original GB potential and is set to 0.3. In the figure, results for two different values of the δ are shown: $\delta = 0$, panel (a), and $\delta = 1.5$, panel (b). We see how the two side-to-side configurations are degenerate for $\delta = 0$ but split into two distinct levels for $\delta > 0$. The end-to-end configurations are also affected by δ but not the T configurations, which remain degenerate.

Therefore, our model represents lipid molecules as two-dimensional elongated objects (on the plane of the monolayer), interacting through anisotropic van der Waals forces. Note that, in our model, interactions between the effective particles do not depend on the phase these particles belong to. This means that the interactions are not sensitive to the chain disorder of molecules in the LE phase as opposed to the perfect chain order in the LC phase. We believe that the impact of this assumption is negligible in view of the fact that our results for the line tension are in reasonable agreement with experiment as commented below.

In addition to the van der Waals interaction, an embedded linear dipole pointing along some direction (not necessarily oriented on the plane) is included. This dipole represents the joint electrostatic charges of the neutral head group of the lipid molecule. The pair potential energy is written as a sum of two contributions, the modified Gay-Berne term and the dipole energy,

$$\Phi(\boldsymbol{r}_{12}, \hat{\boldsymbol{e}}_1, \hat{\boldsymbol{e}}_2) = \Phi_{\rm MGB}(\boldsymbol{r}, \hat{\boldsymbol{e}}_1, \hat{\boldsymbol{e}}_2) + \Phi_{\rm dip}(\boldsymbol{r}, \hat{\boldsymbol{e}}_1, \hat{\boldsymbol{e}}_2). \tag{6}$$

The dipolar energy term is

$$\begin{aligned}\Phi_{\rm dip}(\hat{\boldsymbol{r}}, \hat{\boldsymbol{e}}_1, \hat{\boldsymbol{e}}_2) &= \frac{\mu_\perp^2}{\epsilon_0\epsilon_\perp r^3} + \frac{\mu_\parallel^2}{\epsilon_0\epsilon_\parallel r^3}[\hat{\boldsymbol{e}}_1 \cdot \hat{\boldsymbol{e}}_2 - 3(\hat{\boldsymbol{e}}_1 \cdot \hat{\boldsymbol{r}})(\hat{\boldsymbol{e}}_2 \cdot \hat{\boldsymbol{r}})] \\ &= \frac{\mu_\perp^2}{\epsilon_0\epsilon_\perp r^3} + \frac{\mu_\parallel^2}{\epsilon_0\epsilon_\parallel r^3}(b - 3a_1a_2).\end{aligned} \tag{7}$$

The dipole may have components normal and parallel to the monolayer, respectively, $\mu_\perp = \mu\cos(\pi - \phi) = -\mu\cos\phi$ and $\mu_\parallel = \mu\sin(\pi - \phi) = \mu\sin\phi$, where $\pi - \phi$ is the polar angle of the dipole moment (see Fig. 1). In this dipolar model, we are assuming that the dielectric constants in the two directions $\epsilon_\parallel$ and $\epsilon_\perp$ may be different. Atomistic simulations indicate that angle θ in both LC and LE domains is very close to 22° [20]. As regards the parallel component, it is assumed to be aligned along the long axis of the effective projected particle $\hat{\boldsymbol{e}}$. This assumption is at variance with the results of the latter simulation, which predicts a parallel component that freely rotates in the azimuthal angle, essentially uncorrelated with $\hat{\boldsymbol{e}}$. This result may be a feature of the force field used in the simulations and should be confirmed. In our model, this situation would correspond to setting the in-plane component of the dipole $\mu_\parallel$ to zero. Note that the model does not contemplate the situation where $\hat{\boldsymbol{e}}$ is not on the plane spanned by the dipole moment and the normal to the monolayer.

With this model, we attempt to describe a phase diagram involving two phases, one with orientational disorder (equivalent to the LE phase of the lipid monolayer) and another with orientational order (akin to the LC phase). Also, the effect of the dipolar strength on the coexistence gap can be studied along with the stability and shape of domains and eventually some dynamical aspects of domain growth. Some of these issues are addressed in the present paper. Others will be left for future work.

As formulated, the model is expected to present a number of stable equilibrium phases. Among these are the isotropic phase, where molecules are both spatially and orientationally disordered, and the nematic phase, a fluid phase where molecules are oriented on average along some common

direction called the director. The model also contains an exotic nematic phase, the tetratic, which is a fluid phase with two equivalent directors. The tetratic can replace the standard nematic phase when the aspect ratio of the particles is sufficiently low. Also, the model exhibits a crystalline fully ordered phase at high density. The existence of this sequence of stable phases is based on the known properties of the hard-core interaction of the model, the HR model, which are well known. These and related models have been studied theoretically using mean-field theory [29,30] and by means of simulation [31]. In contrast, the effect of the addition of an anisotropic attractive interaction and a linear dipole has not been investigated. Although the nature of the stable phases is not expected to be modified (based on similar models in two and three dimensions), the effect of the new ingredients will certainly be a profound one. In particular, we would like to obtain some trends as to the effect of the dipole orientation and strength. Initially, we formulate a general model and explore the consequences on phase behavior.

The model is here analyzed using classical DFT and associated mean-field approximations to examine the phase behavior. At this point, we neglect nonuniform spatial ordering since the introduction of this order in the theory gives rise to an unnecessarily complicated numerical problem and, as stated in the Introduction, its contribution to interfacial properties can be neglected. Therefore, at the DFT level, we restrict ourselves to a description of the uniform phases, i.e., isotropic and nematic (we choose the aspect ratio of the particles in such a way as to avoid the stabilization of tetratic ordering, which is certainly not observed in lipid monolayers). These phases will be identified with the LE and LC phases, respectively.

Note again that one crucial assumption of our approach concerns the identification of the phases. The isotropic phase of the model is identified with the LE phase of the monolayer, whereas the nematic phase is meant to represent the LC phase. This may not be a completely realistic representation, especially in the case of the LC phase, but, at least, the model has two essential ingredients: In the LC phase, the aliphatic chains of the molecules are rigid and oriented to optimize the van der Waals energy; and the components of the dipolar moment on the monolayer should be aligned and contribute to a global dipolar moment.

We now formulate a perturbation theory, taking the HR model as a reference system. We write the one-particle density without loss of generality as $\rho(\boldsymbol{r},\hat{\boldsymbol{e}}) = \rho(\boldsymbol{r})f(\boldsymbol{r},\hat{\boldsymbol{e}})$, where $\rho(\boldsymbol{r})$ is the local number density and $f(\boldsymbol{r},\hat{\boldsymbol{e}})$ the orientational distribution function. In the isotropic phase $f(\boldsymbol{r},\hat{\boldsymbol{e}}) = \frac{1}{2\pi}$ since the distribution function has to be normalized

$$\int d\hat{\boldsymbol{e}}\, f(\boldsymbol{r},\hat{\boldsymbol{e}}) = \int_0^{2\pi} d\varphi\, f(\boldsymbol{r},\varphi) = 1. \tag{8}$$

Now the potential energy is split into hard repulsive and attractive parts using a Barker-Henderson scheme [32]. Then, we write a free-energy functional as a sum of ideal and excess parts with the latter containing contributions from the MGB and dipolar terms,

$$F[\rho] = F_{\rm id}[\rho] + F_{\rm HR}[\rho] + F_{\rm MGB}[\rho] + F_{\rm dip}[\rho], \tag{9}$$

where

$$\begin{aligned}\beta F_{\rm id}[\rho] &= \int d\boldsymbol{r} \int d\hat{\boldsymbol{e}}\, \rho(\boldsymbol{r},\hat{\boldsymbol{e}})\{\ln[\rho(\boldsymbol{r},\hat{\boldsymbol{e}})\Lambda^2] - 1\} \\ &= \int d\boldsymbol{r}\, \rho(\boldsymbol{r})\left\{\ln\left[\frac{\rho(\boldsymbol{r})}{2\pi}\Lambda^2\right] - 1 \right. \\ &\quad \left. + \int d\hat{\boldsymbol{e}}\, f(\boldsymbol{r},\hat{\boldsymbol{e}})\ln[2\pi f(\boldsymbol{r},\hat{\boldsymbol{e}})]\right\}\end{aligned} \tag{10}$$

is the ideal free-energy contribution. Λ is the thermal wavelength, and $\beta = 1/kT$. The hard-core contribution can be written as

$$\begin{aligned}\beta F_{\rm HR}[\rho] = \psi_{\rm HR}(\rho_0) \int d\boldsymbol{r}_1 \int d\hat{\boldsymbol{e}}_1 \rho(\boldsymbol{r}_1,\hat{\boldsymbol{e}}_1) \int d\boldsymbol{r}_2 \\ \times \int d\hat{\boldsymbol{e}}_2 \rho(\boldsymbol{r}_2,\hat{\boldsymbol{e}}_2) v_{\rm exc}(\boldsymbol{r}_2 - \boldsymbol{r}_1,\hat{\boldsymbol{e}}_1,\hat{\boldsymbol{e}}_2),\end{aligned} \tag{11}$$

where

$$\begin{aligned}v_{\rm exc}(\boldsymbol{r},\hat{\boldsymbol{e}}_1,\hat{\boldsymbol{e}}_2) &= \left.\begin{cases}1, & r < \sigma_{\rm HC}(\hat{\boldsymbol{r}},\hat{\boldsymbol{e}}_1,\hat{\boldsymbol{e}}_2) \\ 0, & r > \sigma_{\rm HC}(\hat{\boldsymbol{r}},\hat{\boldsymbol{e}}_1,\hat{\boldsymbol{e}}_2)\end{cases}\right\} \\ &= \Theta[\sigma_{\rm HC}(\hat{\boldsymbol{r}},\hat{\boldsymbol{e}}_1,\hat{\boldsymbol{e}}_2) - r]\end{aligned} \tag{12}$$

is the overlap function, and ρ_0 is the mean density. The exact formulation of this functional depends on the hard-core model considered. In the case of HR, scaled-particle theory has been implemented in the past [29], and this is the theory used here. Also,

$$\begin{aligned}F_{\rm MGB}[\rho] = \frac{1}{2}\int d\boldsymbol{r}_1 \int d\hat{\boldsymbol{e}}_1 \rho(\boldsymbol{r}_1,\hat{\boldsymbol{e}}_1) \int d\boldsymbol{r}_2 \int d\hat{\boldsymbol{e}}_2 \rho(\boldsymbol{r}_2,\hat{\boldsymbol{e}}_2) \\ \times \Theta[|\boldsymbol{r}_2 - \boldsymbol{r}_1| - \sigma_{\rm HC}(\hat{\boldsymbol{r}}_{12},\hat{\boldsymbol{e}}_1,\hat{\boldsymbol{e}}_2)] \\ \times \Phi_{\rm MGB}(\boldsymbol{r}_2 - \boldsymbol{r}_1,\hat{\boldsymbol{e}}_1,\hat{\boldsymbol{e}}_2)\end{aligned} \tag{13}$$

is the attractive MGB contribution to the free energy. Finally,

$$\begin{aligned}F_{\rm dip}[\rho] = \frac{1}{2}\int d\boldsymbol{r}_1 \int d\hat{\boldsymbol{e}}_1 \rho(\boldsymbol{r}_1,\hat{\boldsymbol{e}}_1) \int d\boldsymbol{r}_2 \int d\hat{\boldsymbol{e}}_2 \rho(\boldsymbol{r}_2,\hat{\boldsymbol{e}}_2) \\ \times \Theta[|\boldsymbol{r}_2 - \boldsymbol{r}_1| - \sigma_{\rm HR}(\hat{\boldsymbol{r}}_{12},\hat{\boldsymbol{e}}_1,\hat{\boldsymbol{e}}_2)]\Phi_{\rm dip}(\boldsymbol{r}_2 - \boldsymbol{r}_1,\hat{\boldsymbol{e}}_1,\hat{\boldsymbol{e}}_2)\end{aligned} \tag{14}$$

is the dipolar contribution. In this expression, we are assuming that correlations are given by a simple step function (i.e., only the correlation hole is taken into account).

Now, we give some details on how the theory is solved. We only sketch the basic approximations and the numerical approach, considering the more general interfacial case; the thermodynamics of the bulk phases can be obtained from the same interfacial approach using the corresponding bulk distributions. The interfacial structure is computed using a variational method where the density $\rho(x)$ and a set of orientational parameters $\{\Lambda_n(x)\}$ are taken as variational functions. In the context of the present mean-field approach, we do not consider fluctuations of the boundary and, instead, assume a flat boundary. The reference axis x is taken along the boundary normal. This means that the variational parameters $\rho(x)$ and $\{\Lambda_n(x)\}$ will be functions of the x coordinate only. The orientational distribution function is then $f(x,\varphi) = f(\varphi;\{\Lambda_n(x)\})$, where φ is the angle between the long axis of a particle $\hat{\boldsymbol{e}}$ and

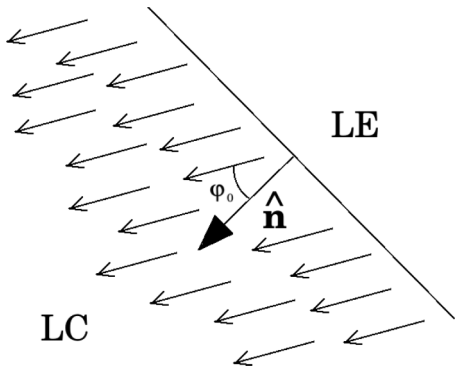

FIG. 3. Definition of angle φ_0 at the boundary between LE and LC domains. Arrows represent the orientation of the local director, which is taken to be uniform in our model. $\hat{\boldsymbol{n}}$ is the unit vector along the inward normal.

the x axis of the laboratory reference frame. The following parametrization is used:

$$f(x,\varphi) = \frac{\exp\left[\sum_{n=1}^{\infty} \Lambda_n(x)\cos\, n(\varphi-\varphi_0)\right]}{\int_0^{2\pi} d\varphi' \exp\left[\sum_{n=1}^{\infty} \Lambda_n(x)\cos\, n\varphi'\right]}. \quad (15)$$

In this expression, we allow for the possibility that, in the nematic phase, the director is oriented at an angle different from the normal direction. This effect is central to our discussion and is taken into account through angle φ_0 in (15), which implies a global rotation of the director, see Fig. 3. The parameters $\{\Lambda_n(x)\}$ at each position x will be a measure of particle ordering about the direction dictated by φ_0. Note that, in this paper, we do not assume a spatial dependence of angle φ_0, which means that the director is uniform across the boundary with no deformation. This assumption is based on our choice of a flat geometry for the boundary and on our inability to tackle the more general problem of boundary deformations and fluctuations within the present formulation. We limit the number of variational parameters to the first two parameters$\Lambda_1(x)$ and $\Lambda_2(x)$, which contain the symmetry of the polar and uniaxial nematic phases. Once the equilibrium values of $\Lambda_1(x)$ and $\Lambda_2(x)$ are obtained, the corresponding local order parameters $s_1(x)$ and $s_2(x)$ in the proper frame (i.e., the frame associated with the nematic director) can be obtained from

$$s_n(x) = \int_0^{2\pi} d\varphi\, f(x;\varphi)\cos\, n(\varphi-\varphi_0). \quad (16)$$

The minimization is realized by discretizing the spatial coordinates, which turns the problem into a minimization problem of a function of many variables, i.e., all the values of ρ, Λ_1, and Λ_2 at the discrete points defined along the x axis. Due to the long-range nature of the dipolar interactions, many such points have to be defined, meaning that the computation box containing the interfacial boundary between the isotropic and the nematic phases will be very long in the direction normal to the boundary. The cutoff in the interactions is set to $30\sigma_0$. We have used a box of length of $100\sigma_0$ in the direction normal to the interface with a grid size of $\Delta x = 0.1\sigma_0$ (the effective box length is, in fact, extended to $160\sigma_0$ to take into account the nonlocal interactions).

Using the property of translational invariance in the direction of the flat boundary (y axis), all integrals over $\boldsymbol{r}_1 = (x_1, y_1)$ and $\boldsymbol{r}_2 = (x_2, y_2)$ in Eqs. (11), (13), and (14) can be written as integrals along x coordinates only. In the process, effective potentials $\tilde{v}_{\rm exc}(x,\varphi_1,\varphi_2)$, $\tilde{\Phi}_{\rm MGB}(x,\varphi_1,\varphi_2)$, and $\tilde{\Phi}_{\rm dip}(x,\varphi_1,\varphi_2)$ are defined, which can be computed in advance. These effective potentials are already integrated on the y coordinates and incorporate the correlation hole given by the Heaviside function. For example, in the case of the dipolar term, we have

$$F_{\rm dip}[\rho] = \frac{L}{2}\int_{-\infty}^{\infty} dx_1 \rho(x_1) \int_{-\infty}^{\infty} dx_2 \rho(x_2) \times \int_0^{2\pi} d\varphi_1 \int_0^{2\pi} d\varphi_2 f[\varphi_1;\Lambda_1(x_1),\Lambda_2(x_1)] \times f[\varphi_2;\Lambda_1(x_2),\Lambda_2(x_2)]\tilde{\Phi}_{\rm dip}(x_1-x_2,\varphi_1,\varphi_2). \quad (17)$$

The factor L, which represents the length of the (flat) boundary, comes by invoking translational invariance along the boundary, which is expressed by the presence of the factor $y_1 - y_2$. The calculation of integrals, such as those in (17), which have the same structure in the case of the other free-energy contributions, involves a serious numerical burden. We must bear in mind that a minimization process over many variables is imposed on the full free-energy functional, and this process involves a very large number of free-energy evaluations.

Our strategy was to evaluate the double angular integrals in a single step before the minimizations. For example, for the dipolar term, we evaluate

$$V_{\rm dip}\left(\Lambda_1^{(1)},\Lambda_2^{(1)},\Lambda_1^{(2)},\Lambda_2^{(2)}\right) \equiv \int_0^{2\pi} d\varphi_1 \int_0^{2\pi} d\varphi_2 \times f[\varphi_1;\Lambda_1(x_1),\Lambda_2(x_1)]f[\varphi_2;\Lambda_1(x_2),\Lambda_2(x_2)] \times \tilde{\Phi}_{\rm dip}(x_1-x_2,\varphi_1,\varphi_2), \quad (18)$$

and create a large table with four entries: The values of two parameters Λ_1, Λ_2 evaluated at the first particle (coordinates with subindex 1) and the values of two parameters Λ_1, Λ_2 evaluated at the second particle (coordinates with subindex 2), i.e., $\Lambda_1^{(1)} \equiv \Lambda_1(x_1)$, $\Lambda_2^{(1)} \equiv \Lambda_2(x_1)$, $\Lambda_1^{(2)} \equiv \Lambda_1(x_2)$, and $\Lambda_2^{(2)} \equiv \Lambda_2(x_2)$. This table is then interpolated for intermediate values of the parameters. The accuracy of this procedure is reasonable [33]. The same procedure is applied to the other free-energy contributions. This strategy saves a lot of computer time and simplifies the interfacial calculations considerably.

The relevant free-energy functional to minimize is the line tension, which is defined as the excess grand potential per unit length $\lambda = (\Omega - \Omega_0)/L$, where $\Omega = F - \mu N$ is the grand potential, L is the interface length, μ is the chemical potential at coexistence, N is the number of particles, and Ω_0 is the bulk grand potential. The line-tension functional is minimized with respect to all the independent variables defined on the discretized x axis, $\rho(x)$, $\Lambda_1(x)$, and $\Lambda_2(x)$ using a conjugate-gradient method. In each case, angle φ_0 between the nematic director and the monolayer normal is fixed at some value in the interval $[0^\circ, 180^\circ]$. This process recovers the bulk results

and bulk coexistence very accurately. However, despite the numerical accuracy of our strategy, very small deviations exist for the bulk properties at different values of φ_0. This is a problem since the computation box is assumed to be coupled to bulk isotropic and nematic phases at each side of the box, and definite coexistence values for density and order parameters, consistent with the numericals of the interfacial problem, have to be fixed as boundary conditions. Any minor difference in the boundary conditions will be detrimental for the correct minimization. The solution is to obtain the bulk coexistence consistently for each value of φ_0, which ensures perfect matching and a smooth minimization process.

For the bulk phases, we assume the dependence $\rho(x) = \rho_0$ and $f(x;\varphi) = f(\varphi)$ for the phase with the lowest symmetry, the nematic phase. In the isotropic phase, $f(\varphi) = 1/2\pi$. In this case, we numerically minimize the total Helmholtz free-energy functional using the same strategy as for the interface. Once the equilibrium (constant) values of the Λ_1 and Λ_2 parameters are obtained for the nematic phase, the order parameters and the equilibrium free energy can be evaluated. From this, the chemical potential and the pressure can be computed numerically, and the whole phase diagram obtained by applying the equal-pressure and equal-chemical potential conditions at each temperature T.

III. RESULTS AND DISCUSSION

For both bulk and interface, three cases have been analyzed: zero dipole, dipole in the plane of the monolayer, and dipole perpendicular to the monolayer. The asymmetry parameter δ is fixed to a value of $\delta = 1.5$. This value gives an energy gap between parallel and antiparallel configurations of 58% (see Fig. 2). As discussed previously, we do not claim this value to be representative of any realistic situation. We simply argue that δ reflects the asymmetry between the two unequivalent configurations of two tilted molecular chains, and that larger tilt angles may reasonably be associated with larger values of δ. A proper connection between the atomistic model and the effective two-dimensional model can be performed but is outside the scope of this exploratory investigation. Larger values of δ, giving stronger energy anisotropies, on the other hand, do not substantially change the results and the qualitative conclusions that can be drawn from the model. In order to check this point, a value of $\delta = 1.75$, giving an energy gap of 69%, was also explored. There is a technical problem with the value of the asymmetry parameter since in the model the value of δ cannot be chosen arbitrarily. For example, for clearly smaller values, the density gap of the isotropic-nematic transition becomes extremely small or even disappears, which is not realistic for the present application. In practice, we have checked that 1.5 is slightly above the limiting value below which a realistic density gap for the isotropic-nematic transition cannot be obtained. What we mean by realistic density gap will be discussed below.

Figure 4 presents four phase diagrams on the temperature-density plane corresponding to the cases mentioned above. All quantities are scaled with the appropriate parameters to give dimensionless quantities, ϵ_{GB} for energies and σ_0 for lengths. In the case of the dipolar strengths, we scale as $\mu_i^* = \mu_i/\sqrt{\epsilon_0\epsilon_i\epsilon_{GB}\sigma_0^3}$ with $i = \parallel, \perp$. All phase diagrams present a common feature: the existence of a transition between an isotropic (LE) phase and a nematic (LC) phase. In all cases, the transition is of first order and preempts the isotropic-vapor transition, which is metastable and below the two isotropic-nematic binodal curves. The latter feature is not a limitation of the model for the present paper, which focuses on the phase coexistence between orientationally ordered and disordered phases. In all cases, the density gap between isotropic and nematic phases rapidly decreases with temperature and eventually closes up, giving rise to a continuous phase transition at a tricritical point. In real monolayers, the density gap disappears at a critical point, above which LC and LE regions can be continuously connected [4]. The different symmetries of the phases involved in our model and the absence of fluctuations in our mean-field treatment preclude the existence of a critical point. Again, this shortcoming is not an essential point for our purposes. Note that, for even higher temperatures, the density gap has to return to a finite value since the infinite-temperature limit of the model is the HR model, which exhibits a first-order transition [29].

We first compare panels (a) and (b) of Fig. 4, both corresponding to zero dipole but for different values of δ. It is clear that an increasing anisotropy, producing a larger energy gap, does not shift the isotropic-nematic transition in temperature but gives rise to an increased density gap. Similar conclusions are drawn from a comparison of panels (a) and (d), corresponding to the same value of δ but to a zero dipole and a purely in-plane dipole, respectively. There exists an incipient isotropic-vapor transition, and the in-plane dipole slightly weakens the anisotropic interactions of the MGB model and promotes the stability of the nematic phase. But, more importantly, the in-plane dipole does not qualitatively affect the phase diagram.

By contrast, the case of a purely perpendicular dipole component, panel (c), is qualitatively different. Condensation of the isotropic phase is clearly discouraged since the perpendicular dipole introduces a purely repulsive interaction. Also, the effective anisotropic interactions promoting the ordering transition decrease with the result that the density gap at a given temperature is considerably reduced, and the tricritical point (not visible at the scale of the other panels) moves to lower temperatures.

Figure 5 presents the line-tension $\lambda(\varphi_0)$ as a function of angle φ_0 between the average projection of the molecular chains in the LC domains (director) and the normal to the phase boundary $\hat{\boldsymbol{n}}$, see Fig. 3. The four panels correspond to the four cases shown in Fig. 4. As a reference, in each case, the value of the temperature is chosen such that the density gap is close or on the same order as that observed in the atomistic simulations [20], which is approximately 27% with respect to the density of the LC phase. Therefore, the temperatures are $kT/\epsilon_{GB} = 0.13$ in panel (a), 0.1825 in panel (b), 0.12 in panel (c), and 0.15 in panel (d), giving density gaps of 27%, 27%, 22%, and 12%, respectively.

The first observation is that the line tension is considerably reduced when dipole interactions, either perpendicular or parallel to the monolayer, are introduced. This reduction cannot be explained alone by the density gap since their values

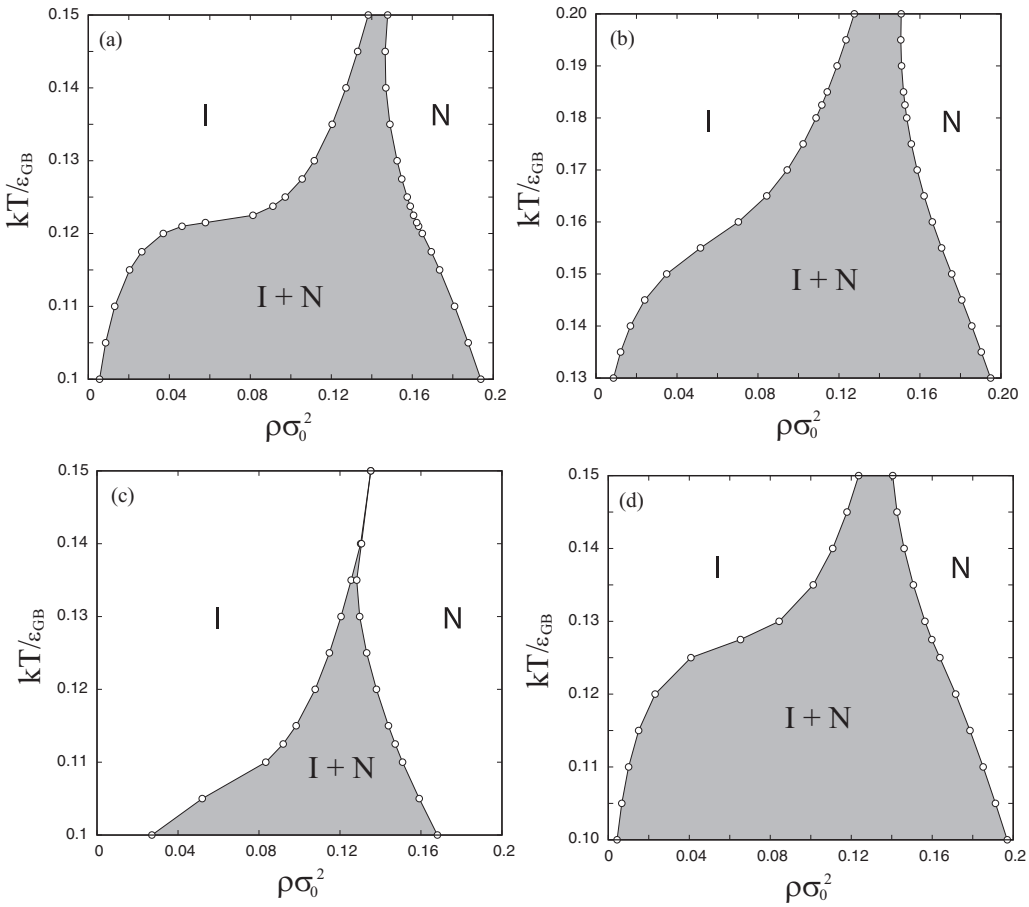

FIG. 4. Phase diagrams for different values of the parameters. (a) $\delta = 1.5,\ \mu_\perp^* = 0,\ \mu_\parallel^* = 0$. (b) $\delta = 1.75,\ \mu_\perp^* = 0,\ \mu_\parallel^* = 0$. (c) $\delta = 1.5,\ \mu_\perp^* = 0.6,\ \mu_\parallel^* = 0$. And (d) $\delta = 1.5,\ \mu_\perp^* = 0,\ \mu_\parallel^* = 0.6$.

are similar, see, e.g., panels (a) and (c). Also, the gap in the order parameters, e.g., the nematic order parameter S_2, at the transition, cannot explain by itself the drop in line tension. The conclusion is that the dipolar interactions are responsible for the substantial reduction in λ. Experimental values of λ for lipid monolayers, extracted from domain size distributions [34], are in the range of 1–10 fN (although values measured using other techniques may be higher by even two orders of magnitude depending on the system [35–37]). Using $\sigma_0 \sim 0.4$ nm (estimated from experimental values of area per lipid in LC domains of DPPC monolayers) and $\epsilon_{GB} \sim 50$ kT (estimated from atomistic force-field simulations [20], and see Ref. [8]), we obtain values of $\lambda \sim 2$–15 fN, i.e., within the same order of magnitude as in Ref. [34].

Interestingly, line tensions exhibit well-defined minima which correspond to equilibrium oblique configurations at the boundary between LE and LC phases. This is indicating the existence of an anisotropic line tension. In cases where no dipole exists, panels (a) and (b), there is a global minimum at $\varphi_0 \simeq 135^\circ$ and a local minimum at $\varphi_0 \simeq 40^\circ$. These two angles are close to being supplementary which means that, in both configurations, the long axes of the effective particles lie on the same straight line, but the projected chains point in opposite directions. The most stable configuration corresponds to chains pointing towards the bulk of LE regions at an angle of $135^\circ - 90^\circ = 45^\circ$ with respect to the boundary. Panel (c) corresponds to a model where a dipole perpendicular to the monolayer is added. Clearly, the barrier between minima is reduced, but the locations of the minima do not change. This indicates that a perpendicular dipole does not affect the anisotropy introduced by the MGB component. Finally, in panel (d), a purely in-plane dipole has been added. In this case, the situation drastically changes as only one minimum is visible at an angle of $\varphi_0 = 90^\circ$. This corresponds to molecular projections parallel to the phase boundary. In all cases, the line tension is anisotropic, meaning that the interface pins the molecular orientation, which is transmitted to the bulk via elastic forces, a situation similar to the anchoring phenomena in liquid crystals.

Another interesting question is the degree of anisotropy of the line tension. A possible measure of the anisotropy ξ is given by the amplitude of its variation in the whole range of φ_0, $\Delta\lambda$, divided by the mean value λ_0, i.e., $\xi = \Delta\lambda/\lambda_0$. In the cases shown in Fig. 5, the values for the anisotropy are $\xi = 0.16,\ 0.22$, and 0.87 in panels (a), (c), and (d), respectively. Dipolar interactions parallel to the monolayer have a profound impact on the line-tension anisotropy, whereas the perpendicular components also add some anisotropy over that of the pure MGB potential which, at $\xi = 16\%$, is already substantial. We are not aware of any experimental values of line-tension anisotropies in lipid monolayers.

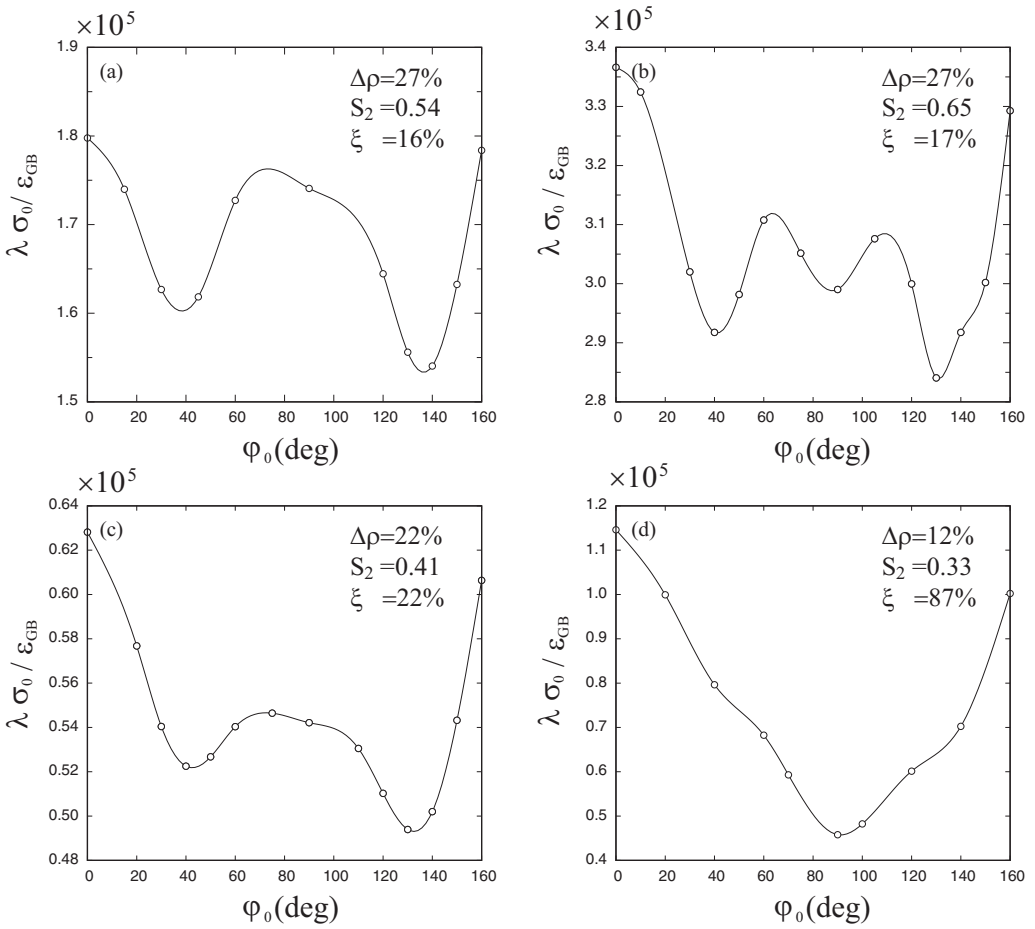

FIG. 5. Line tension as a function of the molecular orientation with respect to the domain boundary normal. (a) $\delta = 1.5,\ \mu_{\parallel}^{*} = 0,\ \mu_{\perp}^{*} = 0\ (kT/\epsilon_{\mathrm{GB}} = 0.13)$, (b) $\delta = 1.75,\ \mu_{\parallel}^{*} = 0,\ \mu_{\perp}^{*} = 0\ (kT/\epsilon_{\mathrm{GB}} = 0.1825)$. (c) $\delta = 1.5,\ \mu_{\parallel}^{*} = 0,\ \mu_{\perp}^{*} = 0.6\ (kT/\epsilon_{\mathrm{GB}} = 0.12)$. (d) $\delta = 1.5,\ \mu_{\parallel}^{*} = 0.6,\ \mu_{\perp}^{*} = 0\ (kT/\epsilon_{\mathrm{GB}} = 0.15)$. The continuous line is a cubic spline fitting intended only as a guide to the eye.

These results should be compared with available evidence on molecular structure and ordering. An important source of information comes from atomistic computer simulations. Two such simulations on DPPC monolayers have recently been published [20,21]. The two use the same force fields, and the only difference is system size. We focus on Ref. [21] in which complete phase separation was probed along the coexistence region, and pictures of representative molecular configurations were shown. Invariably, an angle φ_0 at the domain boundaries different from 90° can be seen in the configurations. Direct visual estimates of the angle provide a value of ∼30° (see panel 3, Fig. 2 of Ref. [21]).

The above results imply that the in-plane dipolar component cannot be large or, at least, cannot influence the structural properties of the domain. This is supported by the results of Ref. [20] that the in-plane component of the dipoles show almost complete rotational motion about the monolayer normal. This could imply that the in-plane dipolar components of neighboring molecules interact weakly because of strong screening [38] or otherwise. Therefore, the only relevant or effective dipolar component would be the perpendicular one. The line tension is strongly affected by this component, which reduces its value. The angular anisotropy of the line tension, which is otherwise contained in the model with no dipole interactions, increases moderately when perpendicular dipole forces are present. Therefore, the main contribution to the anisotropy is due to the molecular tilt; the perpendicular dipoles contributing to a lesser extent. The angular dependence of the line tension can be represented by

$$\lambda(\varphi_0) = \lambda_0 + \sum_{n=1}^{\infty} \lambda_n \cos n\varphi_0. \tag{19}$$

The different behaviors shown in Fig. 5 can be explained in terms of the $n = 1$–4 components. Minima at $\simeq 45°$ and 135° are due to the $n = 4$ term. The $n = 1$ and 3 components affect the relative stability of these two minima. The minimum at 90° is due to the $n = 2$ component. A model potential with no gap between ↑↑ and ↑↓ configurations promotes a 90° angle at the boundary [39] (planar orientation). In-plane dipoles also favor this configuration. The presence of a tilt-induced energy gap is responsible for the preferred orientations at oblique angles.

Competition between bulk interactions from perpendicular dipoles and an isotropic line-tension λ_0 has been invoked as a mechanism to determine domain shape in mesoscopic models [13–17]. Dipole interactions promote elongated shapes, whereas an isotropic line tension favors circular domains. Different shape regimes emerge from this competition. However, the angle-dependent terms (19), which are present even in the absence of dipolar interactions, play the same role as these

interactions. In this alternative scenario, long linear sectors of the domain boundary would optimize the line free energy, thus, favoring the formation of elongated domains with long linear boundaries. In fact, the results presented in this section correspond to a value of the line-tension-to-dipolar strength ratio of $\Lambda = \lambda_0^*/(\mu_\perp^* \Delta\rho^*)^2 \simeq 0.02$, i.e., to a regime dominated by dipolar interactions. A reduction of $\mu_\perp^*$ to 0.1 would increase Λ to $\sim$1. Even in this case, domains with a high number of lobes are stabilized, according to mesoscopic models [13,16,17]. Anisotropic line tensions are expected to suppress or, at least, reduce the stability of these highly lobed structures in favor of shapes with lower overall curvature. Other factors, such as nematic director distortion, and possible defects in the director field, may also play a role in the final free-energy balance.

IV. SUMMARY AND CONCLUSIONS

In this paper, we have formulated a very simple model to study the interfacial structure at the boundary between LC and LE domains in DPPC monolayers. The model predicts an anisotropic line-tension $\lambda(\varphi_0)$ with respect to angle φ_0 between the nematic director (which describes orientation of the projected molecular chains in LC domains) and the normal to the boundary. The minimum line tension occurs at oblique angles, which is in agreement with results from atomistic simulation [20,21]. Anisotropy in the line tension is already implicit in a model with only van der Waals lipid chain interactions (modified Gay-Berne potential), and dipolar components perpendicular to the monolayer only marginally increase the anisotropy. Indirectly, our model also supports the concept that in-plane dipolar components should play a minor role since these components favor a planar orientation at the boundary, which is incompatible with the results from atomistic simulations. This may be explained by the stronger screening of in-plane dipoles as compared to perpendicular dipoles. This conclusion supports the commonly accepted assumption made in previous mesoscopic models [13–17].

Our results indicate that theoretical mesoscopic models aimed at predicting domain shape and domain shape transitions should be extended to account for anisotropy in the line tension. On one hand, in-plane dipolar components may not be relevant to construct realistic models (see Ref. [38] where the effect of such contributions is discussed). On the other, models with perpendicular dipoles should also reflect the anisotropy in the line tension stemming from the combined effect of nonzero tilt angles of lipid chains and perpendicular dipoles. We should recall that all atomistic simulations to date consistently predict nonzero lipid-chain tilt angles in LC domains [20,21,40]. In our model, the perpendicular dipole component seems to play an important role in reducing the line tension but only induces a small incremental anisotropy. Of course, competition between (long-range) dipolar bulk interactions and line tension is a relevant factor for the global domain morphology as indicated by mesoscopic models [13–17]. But an anisotropic line tension competing with dipolar energy and an elastic energy associated with director distortion [23,41] together with the possible excitation of defects or grain boundaries [5] may be a crucial requirement.

ACKNOWLEDGMENTS

We acknowledge financial support from Grants No. FIS2017-86007-C3-1-P and No. FIS2017-86007-C3-2-P from Ministerio de Economía, Industria y Competitividad (MINECO) of Spain.

[1] J. Pérez-Gil, N. Wüstneck, A. Cruz, V. B. Fainerman, and U. Pison, Adv. Colloid Interface Sci. **117**, 33 (2005).
[2] C. Casals and O. Cañadas, Biochim. Biophys. Acta, Biomembr. **1818**, 2550 (2012).
[3] V. M. Kaganer, H. Möhwald, and P. Dutta, Rev. Mod. Phys. **71**, 779 (1999).
[4] L. K. Nielsen, T. Bjørnholm, and O. G. Mouritsen, Langmuir **23**, 11684 (2007).
[5] U. Bernchou, J. Brewer, H. S. Midtiby, J. H. Ipsen, L. A. Bagatolli, and A. C. Simonsen, J. Am. Chem. Soc. **131**, 14130 (2009).
[6] S. Choe, R. Chang, J. Jeon, and A. Violi, Biophys. J. **95**, 4102 (2008).
[7] H. Dominguez, A. M. Smondyrev, and M. L. Berkowitz, J. Phys. Chem. B **103**, 9582 (1999).
[8] J. Israelachvili, *Intermolecular and Surface Forces* (Academic, London, 1992).
[9] H. Möhwald, Annu. Rev. Phys. Chem. **41**, 441 (1990).
[10] G. Ma and H. C. Allen, Langmuir **22**, 5341 (2006).
[11] H. Hauser and M. C. Phillips, in *Progress in Surface and Membrane Science* 13, edited by J. F. Danielli, M. D. Rosenberg, and D. A. Cadenhead (Academic, New York, 1979).
[12] J. Miñones, Jr, J. M. Rodríguez Patino, O. Conde, C. Carrera, and R. Seoane, Interface. Col. Surf. Sci. A: Physicochem. Eng. Aspects **203**, 273 (2002).
[13] V. T. Moy, D. J. Keller, H. E. Gaub, and H. M. McConnell, J. Phys. Chem. **90**, 3198 (1986).
[14] D. J. Keller, J. P. Korb, and H. M. McConnell, J. Phys. Chem. **91**, 6417 (1987).
[15] M. Iwamoto, F. Liu, and Z.-C. Ou-Yang, J. Chem. Phys. **125**, 224701 (2006).
[16] M. Iwamoto, F. Liu, and Z.-C. Ou-Yang, Eur. Phys. Lett. **91**, 16004 (2010).
[17] F. Campelo, A. Cruz, J. Pérez-Gil, L. Vázquez, and A. Hernández-Machado, Eur. Phys. J. E **35**, 49 (2012).
[18] J. H. Ipsen, O. G. Mouritsen, and M. J. Zuckermann, J. Chem. Phys. **91**, 1855 (1989).
[19] O. G. Mouritsen and M. J. Zuckermann, Chem. Phys. Lett. **135**, 294 (1987).
[20] E. Velasco and L. Mederos, arXiv:1903.09554.
[21] M. Javanainen, A. Lamberg, L. Cwiklik, I. Vattulainen, and O. H. Samuli Ollila, Langmuir **34**, 2565 (2018).
[22] The idea of assuming that order in LC domains can be assimilated to nematic order has been exploited before. See, for example, Ref. [23] in the case of lipid monolayers and J.-B. Fournier, and P. Galatola, Braz. J. Phys. **28**, 329 (1998) in the case of bilayers.
[23] I. Sriram and D. K. Schwartz, Surf. Sci. Rep. **67**, 143 (2012).
[24] A. M. Bohle, R. Hołyst, and T. Vilgis, Phys. Rev. Lett. **76**, 1396 (1996).

[25] J. G. Gay and B. J. Berne, J. Chem. Phys. **74**, 3316 (1981).
[26] D. J. Adams, G. R. Luckhurst, and R. W. Phippen, Mol. Phys. **61**, 1575 (1987).
[27] E. de Miguel, L. F. Rull, M. K. Chalam, and K. E. Gubbins, Mol. Phys. **74**, 405 (1991).
[28] E. Velasco, A. M. Somoza, and L. Mederos, J. Chem. Phys. **102**, 8107 (1995).
[29] Y. Martínez-Ratón, E. Velasco, and L. Mederos, J. Chem. Phys. **122**, 064903 (2005).
[30] Y. Martínez-Ratón, E. Velasco, and L. Mederos, J. Chem. Phys. **125**, 014501 (2006).
[31] A. Donev, J. Burton, F. H. Stillinger, and S. Torquato, Phys. Rev. B **73**, 054109 (2006).
[32] J.-P. Hansen and I. R. McDonald, *Theory of Simple Liquids* (Academic, New York, 1986).
[33] Several checks were performed by using different grid sizes and interpolation radii in order to reach a compromise between accuracy and numerical burden. With our choice of interpolation parameters, the conjugate-gradient procedure used to minimize the free energy produced values of the gradient, at the end of the minimization, of order 10^{-5} per grid point.
[34] D. W. Lee, Y. Min, P. Dhar, and A. Ramachandran, J. N. Israelachvili, and J. A. Zasadzinski, Proc. Natl. Acad. Sci. USA **108**, 9425 (2011).
[35] B. L. Stottrup, A. M. Heussler, and T. A. Bibelnieks, J. Phys. Chem. B **111**, 11091 (2007).
[36] D. J. Benvegnu and H. M. McConnell, J. Phys. Chem. **96**, 6820 (1992).
[37] S. Wurlitzer, P. Steffen, and T. M. J. Fischer, J. Chem. Phys. **112**, 5915 (2000).
[38] H. M. McConnell and V. T. Moy, J. Phys. Chem. **92**, 4520 (1988).
[39] Y. Martínez-Ratón, Phys. Rev. E **75**, 051708 (2007).
[40] D. Mohammad-Aghaie, E. Macé, C. A. Sennoga, J. M. Seddon, and F. Bresme, J. Phys. Chem. B **114**, 1325 (2010).
[41] D. Pettey and T. C. Lubensky, Phys. Rev. E **59**, 1834 (1999).